Article

Remote Sensing Evaluation of Trophic Status in the Daihai Lake Based on Fuzzy Classification

Fang Wang [1], Song Qing [1,2,3,*], Chula Sa [1], Quan Lai [1] and An Chang [1]

1 College of Geographic Science, Inner Mongolia Normal University, Hohhot 010022, China;
   20236016010@mails.imnu.edu.cn (F.W.); sachula@imnu.edu.cn (C.S.); laiquan@imnu.edu.cn (Q.L.);
   changan1978@126.com (A.C.)
2 Applied Mathematics Center of Mongolia Autonomous Region, Hohhot 010022, China
3 The Key Laboratory of Infinite-Dimensional Hamiltonian System and Its Algorithm Application,
   Inner Mongolia Normal University, Ministry of Education, Hohhot 010022, China
* Correspondence: qingsong@imnu.edu.cn

Abstract: Trophic state index (TSI) is a critical ecological and environmental issue in water resource management that has garnered significant attention. Given the complexity of optical characteristics in aquatic environments, this study employs fuzzy classification methods (FCM) and composite nutrient status indices to meticulously classify in-situ remote sensing reflectance data, aiming to develop evaluation models for different nutrient status categories to facilitate the assessment of the Daihai River in Inner Mongolia, China. Subsequently, we applied this model to MSI data to analyze the nutrient status of Daihai Lake from 2016 to 2021. Furthermore, a structural equation model (SEM) was utilized to explore the primary driving factors influencing nutrient status. The results indicated that the water bodies in Daihai Lake can be broadly classified into three categories, with the nutrient status models demonstrating robust performance for each category ($R^2 = 0.80$, $R^2 = 0.83$, and $R^2 = 0.74$). Comparisons were made between nutrient status accuracies obtained through the NCM and FCM based on measured data, yielding R^2 values of 0.74 and 0.85, respectively. Furthermore, the TSI results derived from MSI inversion were validated, with NCM achieving an R^2 of 0.49, RMSE of 6.88, and MAPE of 10.36%, while FCM exhibited an R^2 of 0.55, RMSE of 8.89, and MAPE of 13.18%. An SEM–based analysis revealed that over the long term, human activities exerted a more substantial impact on eutrophication in Daihai Lake, while climatic factors played an accelerating and reinforcing role. These results are consistent with prior research in the Daihai area, indicating a state of mild eutrophication and the potential of the fuzzy classification method and comprehensive trophic status index method in eutrophication assessment.

Keywords: trophic status; Daihai Lake; fuzzy classification; Sentinel-2

1. Introduction

Trophic status refers to the process by which the accumulation of excessive nutrients in water leads to a transition in productivity from low to high [1], this process exhibits high spatiotemporal variability [2]. The enrichment of nutrients is an intrinsic mechanism that alters the original nutrient status, thereby affecting water quality and leading to a series of issues, such as eutrophication [3]. This can trigger recurrent algal blooms and significant mortality of aquatic flora and fauna, thereby disrupting the aquatic ecosystem, impeding rational water resource utilization, and potentially posing a threat to the longevity of lakes [4]. However, traditional methods face various limitations in terms of spatial and temporal scales, as well as in human and material resources. The emergence of remote sensing technology not only addresses these shortcomings but also achieves significant advancements in the integration of methods for temporal scale analysis, spatial analysis, and the assessment of trophic status.

In 1977 Carlson devised an indicator index for evaluating the nutritional state of water bodies, using algal biomass as a key index [5]. Subsequently, methods for estimating nutritional status based on predictive equations between parameters have emerged. Current remote sensing assessments of trophic status primarily employ the following methodologies. (1) Remote sensing reflectance (Rrs) and trophic state index (TSI) empirical models. This approach involves applying the correlation between status indices and single-band [6,7], band ratios [8,9], or band combinations [10,11] of remote sensing reflectance. Owing to limitations in accurately assessing trophic status with single indicators, researchers have investigated the evaluation of trophic status in complex water bodies by combining multiple parameters [9–18]. Existing inversion models may be challenging to apply to different unmeasured lakes because models calibrated from limited field data may only be applicable to sampled water bodies and similar conditions [19]. (2) Absorption coefficient and TSI empirical models. The absorption coefficient of optically active substances in water contains all the TSI component information. Using remote sensing absorption coefficients to assess TSI can effectively reduce the cumulative errors [20–22]. However, the applicability of this method is relatively low in northern lakes dominated by Colored Dissolved Organic Matter (CDOM) [21]. (3) Grading models are based on water parameters, water color indices, and remote sensing reflectance. Through the correlation between these parameters, classification, grading, and scoring can determine the nutritional status level or type of the water body [23–27]. (4) Latest method. Researchers have developed various methods to assess the trophic status of water bodies, including the Algal Biomass Index (ABI) [28], the Forel–Ule Index (FUI) [19]. Additionally, by analyzing long–term changes in land use and land cover (LULC), studies have explored how human activities affect water quality, trophic status, and biodiversity, highlighting the complex relationship between ecosystem services and anthropogenic activities [29]. Moreover, machine learning and deep learning algorithms have been employed to classify and predict water quality categories, enabling more precise trophic status assessments [30].

Optical classification is known to enhance the retrieval capabilities in optically complex water bodies [31]. Optical classification methods offer a viable solution for the challenge of remote sensing signal inversion in complex water bodies [32]. Bao et al.(2015) [33] and Zhang et al.(2015) [34] proposed a method for estimating chlorophyll a concentration (Chla) based on hard classification. However, the use of hard clustering methods can lead to non-uniformity in the classification results of optical properties, resulting in discontinuities in the estimates of Chla concentration [35]. Therefore, a soft classification–based method for estimating Chla concentration has been developed [36–38]. The fuzzy clustering, also referred to as soft classification, aims to mitigate the sharp boundaries inherent in hard clustering by utilizing "membership degrees" to delineate distinctions between various types of water bodies [39]. The soft classification method has attracted increasing attention due to its ability to define the central spectrum of each class through fuzzy classification, calculate the distance weights between each spectrum and the central spectra, and maintain continuity in the estimation results [35–38]. Moreover, the fuzzy–based classification method employing remote sensing reflectance is fundamentally independent of specific regions and timeframes, indicating enhanced universality and potential for large-scale applications compared with prior regional approaches [40].

Although optical classification–based grouping and algorithm development offer notable advantages, there is currently no reported utilization of optical classification for assessing lake nutritional status. In this study, we devised a novel algorithm utilizing soft classification techniques to estimate the Trophic State Index by leveraging Sentinel–2 MSI data from the highly turbid and eutrophic Daihai Lake. This study aimed to achieve the following objectives: (1) to perform optical classification of Daihai Lake by employing a soft-classification approach, (2) to develop a soft-classification-based algorithm for assessing the nutrient status of Daihai Lake and validate the accuracy of the algorithm, and (3) to analyze the spatiotemporal variations and underlying drivers of trophic status in Daihai Lake from 2016 to 2021.

2. Materials

2.1. Study Area

Daihai Lake is located in the southeastern part of Liangcheng County, Ulanqab City, Inner Mongolia Autonomous Region, China (40°29′07″–40°37′06″ N, 112°33′31″–113°46′40″ E), representing a characteristic graben-style tectonic basin (Figure 1) [41]. The lake faces challenges in terms of water supply [42] and has experienced numerous expansions and contractions due to tectonic shifts and historical climate fluctuations [43]. Positioned in the sensitive region of northern China, Daihai experiences a mid-temperate, semi–arid, continental monsoon climate. This unique natural geographical setting enhances the fragility of the lake wetland ecosystem in Daihai [44]. As the third largest inland lake in the Inner Mongolia Autonomous Region, Daihai plays a vital role in climate regulation, ecological restoration, and water conservation, serving as a pivotal component of ecological security in northern China [44]. General Secretary Xi Jinping has expressed concerns about the environmental state of Daihai's water body and has emphasized the importance of comprehensive ecological management and effective implementation during the 13th National People's Congress. Currently, the emergency water replenishment project, "Bringing Water from the Yellow River to Daihai", is scheduled for official implementation in 2023. Over the years, due to the intervention of climate change and human activities in the watershed, the lake's water level has continuously declined, and the lake surface has been shrinking. This has led to a deterioration in water quality, resulting in an increasingly prominent issue of eutrophication [41].
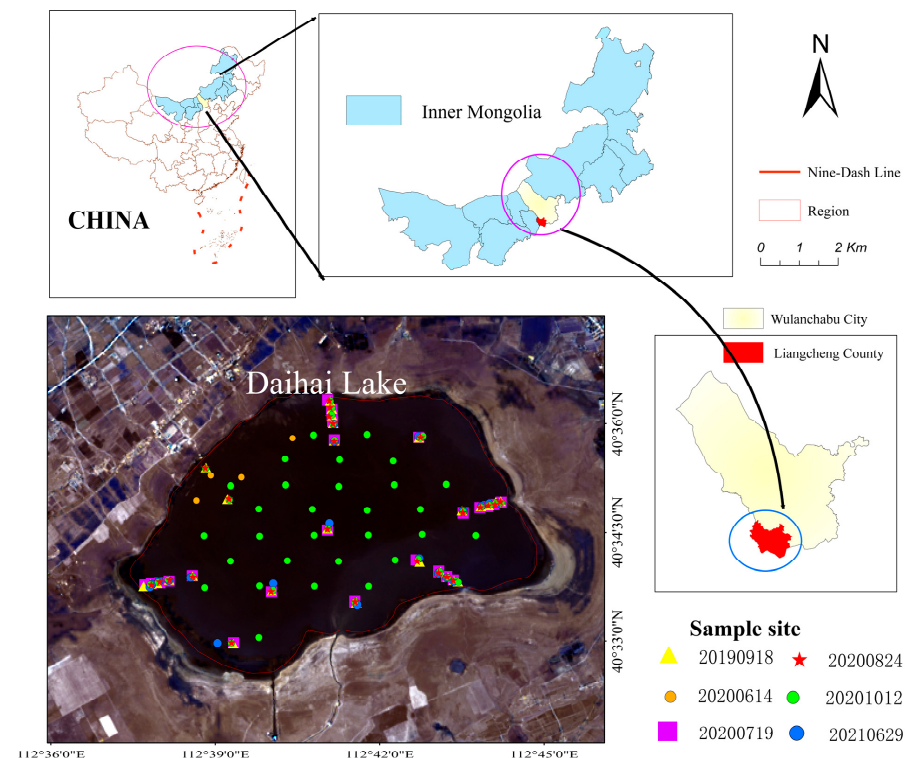

Figure 1. Locations of the Daihai Lake and sampling sites.

2.2. In Situ Measurements

Six field surveys were conducted in the Daihai water area on 14 June, 21 July, 24 August, 12 October 2020, and 18 September 2019, 29 June 2021. The "water method" [45] was employed to capture water surface spectra, while transparency was measured on-site using a Secchi disk [46]. Water samples were collected from the surface, preserved at low temperatures, and subsequently analyzed in the laboratory for chlorophyll concentration using spectrophotometry [47]. A total of 156 datasets were obtained.

2.3. Sentinel-2 MSI Data

For the trophic status assessment of water bodies, trophic status inversion can be conducted using Sentinel–2 Multi–Spectral Instrument (MSI) data. Sentinel–2 images were obtained from the official European Space Agency website (https://scihub.copernicus.eu/, accessed on 7 September 2021). The two satellites yielded a 5–day revisit period, providing remote sensing data with high spatial and temporal resolutions [48]. We obtained atmospheric apparent reflectance remote sensing data for the Daihai area from 2016 to 2021, comprising a total of 84 Sentinel–2 images to capture the long–term temporal dynamics of the Daihai water body. Among these, three Sentinel–3 images were selected to align with the dates of the field surveys: 14 June 2020, 21 July 2020, and 12 October 2020. These images were used to validate the accuracy of the nutrient status remote sensing inversion for the Daihai water body.

The accurate extraction of water body information from remote sensing images requires high–quality atmospheric correction. In this 76 study, we employed the C2RCC method for the atmospheric correction of Sentinel–2 Level 1c data. The C2RCC processor is a versatile ocean color processor tailored for intricate Case 2 waters [49] and has demonstrated commendable performance across various sensors in similar environments [50]. This processor relies on a radiative transfer simulation database calibrated using neural networks anchored by five sets of inherent optical properties [51].

2.4. Other Data

Meteorological data, including air temperature, precipitation, and wind speed for the years 2016 to 2020, were sourced from the Liangcheng Meteorological Station via the China Meteorological Information Center (http://data.cma.cn, accessed on 7 September 2021). These data were used to investigate the relationship between lake nutrient status and meteorological factors. Given the presence of an ice–covered period in Daihai, the monthly average values for the interval from April to October, as well as the annual averages, were utilized for meteorological analysis.

Agricultural and industrial data for Liangcheng County, Ulanqab City, spanning 2016 to 2020, were extracted from the Inner Mongolia Statistical Yearbook. We selected crop sowing area, grain production, and gross domestic product (GDP) as agricultural data. The industrial data include information from the primary, secondary, and tertiary sectors.

3. Methods

The primary research framework depicted in Figure 2 comprises three main components. (1) Conducting optical classification of water bodies. First, actual measurement data of Daihai water were collected. The Fuzzy C–Means (FCM) method was utilized to conduct an optical classification of the spectral data of the water body, followed by an analysis of the characteristics of each class. (2) Construction of a trophic state assessment model. Optimal band ratios were selected to implement the assessment models for each class. This included the principal assessment model based on the FCM method as well as a model established without classification. An accuracy evaluation is performed for these models. (3) Model application. C2RCC atmospheric correction and accuracy assessment was performed on remote sensing images. The accuracy of remote–sensing inversion for the trophic status of the Daihai water body was also validated. Subsequently, the application of the soft–classification–based nutrient status assessment model was utilized for Daihai time–series data spanning 2016 to 2021. The spatiotemporal distribution patterns for the water body were derived, followed by an analysis of the driving factors, including meteorological, agricultural, and industrial influences, using a structural equation model.
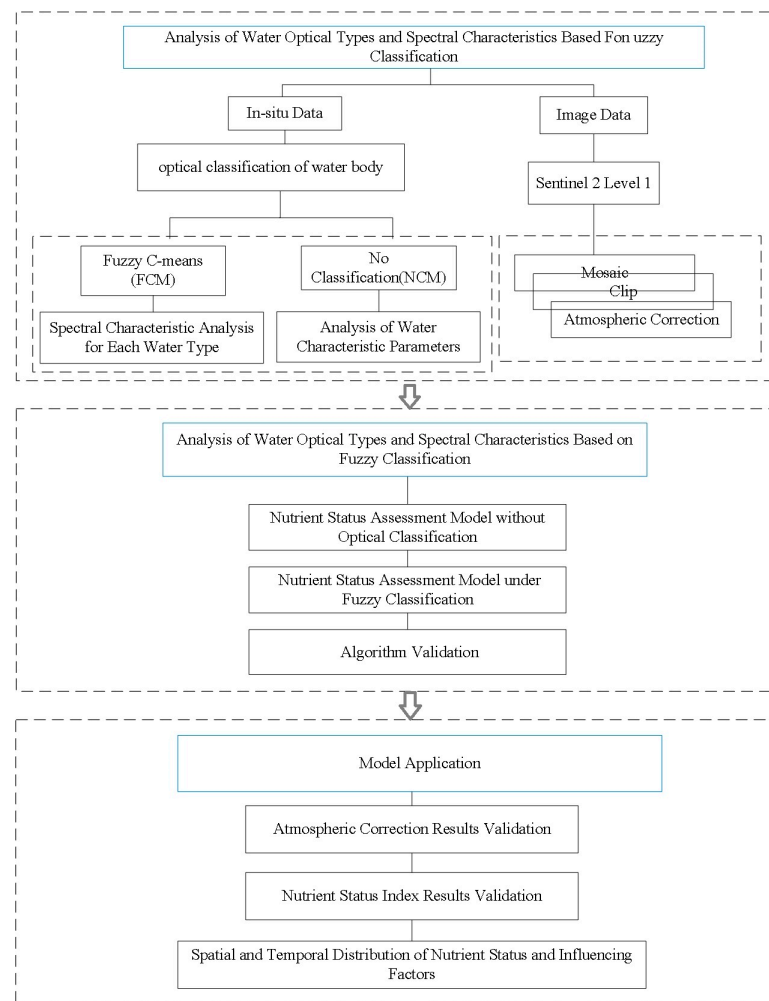
Figure 2. Flow chart of the study process.

3.1. Trophic State Index: TSI

Eutrophication is a significant concern for inland lake management. This study employed the Comprehensive Trophic State Index (TSI) method proposed by Carlson in 1977 [5] to evaluate the eutrophication status of the Daihai water body. This method represents an enhanced iteration of Carlson's *TSI*, primarily relying on weighted averages for computation. The resulting trophic state index was conventionally normalized within a range of 0–100, where *TSI* $\geq$ 50 denotes eutrophication, 50 $\geq$ *TSI* $\geq$ 30 indicates mesotrophy, and *TSI* < 30 signifies oligotrophy. The specific formula is as follows:

$$TSI = \sum_{j=1}^{n} W_j \times TSI(j) \tag{1}$$

$$W_j = \frac{r_{ij}^2}{\sum_{j=1}^{n} r_{ij}^2} \tag{2}$$

$$TSI(SDD) = 10 \times (5.118 - 1.086 * InSDD) \tag{3}$$

$$TSI(Chla) = 10 \times (2.500 + 1.086 * InChla) \tag{4}$$

In this study, calculations were performed based on transparency, where "r^2_j" represents the coefficient of determination between the *SDD* (Secchi disk depth) and parameter "*j*", which can be either the *SDD* or Chlorophyll-a concentration and *Wj* is the corresponding. The specific values were $r^2_{SDD} = 1$ and $r^2_{Chla} = 0.06$. "n" = 2 indicates the number of parameters utilized.

3.2. Fuzzy C-Means Algorithm

This study employed FCM algorithm for clustering analysis on a dataset comprising 156 sets of field–measured remote–sensing Rrs data. FCM, an enhancement of the conventional C-means algorithm (HCM) [52], is a more adaptable fuzzy partitioning method. Unlike hard clustering methods, FCM facilitates the assignment of data points to multiple cluster centers, expressing their association with each cluster through varying membership degrees. This flexibility enables FCM to handle real–world scenarios in which data may be indistinct, ambiguous, or pertaining to multiple categories. Among the various fuzzy algorithms, FCM is prevalent because of its widespread use and effectiveness. It autonomously categorizes samples by optimizing the objective function to ascertain the membership degree of each sample to each class center [53]. The general steps of the soft classification method are outlined as follows:

(1) Data preparation: Collect and organize the dataset required for the soft classification.
(2) Determine the number of clusters (m): The desired number of clusters for soft classification was established based on problem–specific requirements or domain knowledge.
(3) Initialize the membership matrix: Assign initial membership values to each data point either randomly or based on the preliminary information. Each element in the membership matrix typically represents the degree of membership of a data point to a specific cluster center.
(4) Compute cluster centers (c): Calculate the positions of each cluster center using the current membership matrix.
(5) Update the membership matrix: Compute a new membership matrix based on the current cluster centers. The membership values were updated according to the distances between the data points and each cluster center. The Euclidean method was employed for the distance calculation.
(6) Repeat iterations of Steps 4 and 5: The process was iterated by recalculating the cluster centers and updating the membership matrix until a specified stopping criterion was met, such as reaching the maximum number of iterations or when the change in cluster centers fell below a predefined threshold. The iterative process aims to optimize and approach the objective function progressively.
(7) Output the clustering results: The final membership matrix was used to assign each data point to its respective cluster center, yielding the ultimate soft clustering result.

In addition, this algorithm facilitates the initialization of the cluster centers prior to commencing the iteration process. The FCM algorithm, as a partition–based clustering approach, attempts to maximize the similarity within clusters and minimize the similarity between distinct clusters [54,55].

3.3. TSI Retrieval Algorithm

An optimal band ratio–based model was established to assess the nutrient status tailored to each water body type classified using the FCM method.

$$\text{TSI}_{Modeli} = a \times \text{Rrs}(\lambda_i) / \text{Rrs}(\lambda_j) + b \tag{5}$$

where $\text{Rrs}(\lambda_i)$ and $\text{Rrs}(\lambda_j)$ represent the remote sensing reflectance in the visible light bands. TSI_{Model1}, TSI_{Model2}, and TSI_{Model3} are models established for each type of water body, and a and b denote the model coefficients.

3.4. Structural Equation Model

This study employed structural equation modeling (SEM) to analyze the spatiotemporal variations in nutrient status within Daihai, attributed to factors such as climate, agriculture, and industry. The influence factor data spanning from 2016 to 2020 were standardized using Z–scores in SPSS software 24. Subsequently, an SEM was constructed using Amos 24.0, to assess the respective impacts of these three factors on eutrophication of the Daihai water body.

3.5. Accuracy Metrics

This study assessed the performance of nutrient status algorithms across various optical water types, estimating model accuracy through metrics including the Root Mean Square Error (*RMSE*), Mean Absolute Percentage Error (*MAPE*), and Coefficient of Determination (R^2). The specific formulas used are as follows:

$$RMSE = \sqrt{\frac{1}{N}\sum_{i=1}^{N}\left(x_{imea} - x_{ipre}\right)^2} \qquad (6)$$

$$MAPE = \frac{1}{N}\sum_{i=1}^{N}\frac{\left|x_{imea} - x_{ipre}\right|}{x_{imea}} * 100\% \qquad (7)$$

$$R^2 = \frac{\sum_{i=1}^{N}\left(x_{imea} - \bar{x}\right)\left(y_{ipre} - \bar{y}\right)}{\sqrt{\sum_{i=1}^{N}\left(x_{imea} - \bar{x}\right)^2 \sum_{i=1}^{N}\left(y_{ipre} - \bar{y}\right)^2}} \qquad (8)$$

where N represents the number of samples; and x_{imea} and x_{ipre} represent the measured and estimated values, respectively.

4. Results

4.1. Water Optical Types

Based on the shape and distance of Rrs, 156 spectral samples were divided into three clusters using cluster analysis (Figure 3). Figure 3a represents the aggregate reflectance, while Figure 3b displays the centroid reflectance spectra for each cluster. Figure 3c–e show the reflectance spectra of the three clusters. All water body types exhibited similar magnitudes and spectral characteristics those to of the Rrs. The low reflectance and high absorption in the blue wavelength range (400–500 nm) are characteristic of inland water bodies [56]. As show in Figure 3 differences among optical water types primarily arose in the magnitude of reflectance and spectral profile within the 600–700 nm range. Cluster 1, with the fewest samples, generally exhibited higher remote sensing reflectance values. Cluster 2 and Cluster 3 comprised 54 and 93 samples, respectively. The range of remote sensing reflectance values gradually decreased from Cluster 1 to Cluster 3. Additionally, Cluster 3 lacked a prominent peak at 670 nm and displayed a smaller peak at 800 nm than Clusters 1 and 2. The reflectance spectra of the three clusters in Figure 3e exhibited no substantial shape variations, although the peaks were slightly shifted towards higher wavelengths.

4.2. Evaluation of TSI Inversion Results Based on Measured Data

In the non-classification scenario (NCM), the ratio of Rrs (665) to Rrs (490) was selected as the dependent variable for model construction, yielding the equation y = −44.58 ∗ x + 103.23. Within the fuzzy classification framework, three distinct models were formulated using different band ratios, Rrs (665)/Rrs (443), Rrs (665)/Rrs (490), and Rrs (705)/Rrs (490), each contributing to the construction of simple linear models, as detailed in Table 1.

Table 1. TSI evaluation model.

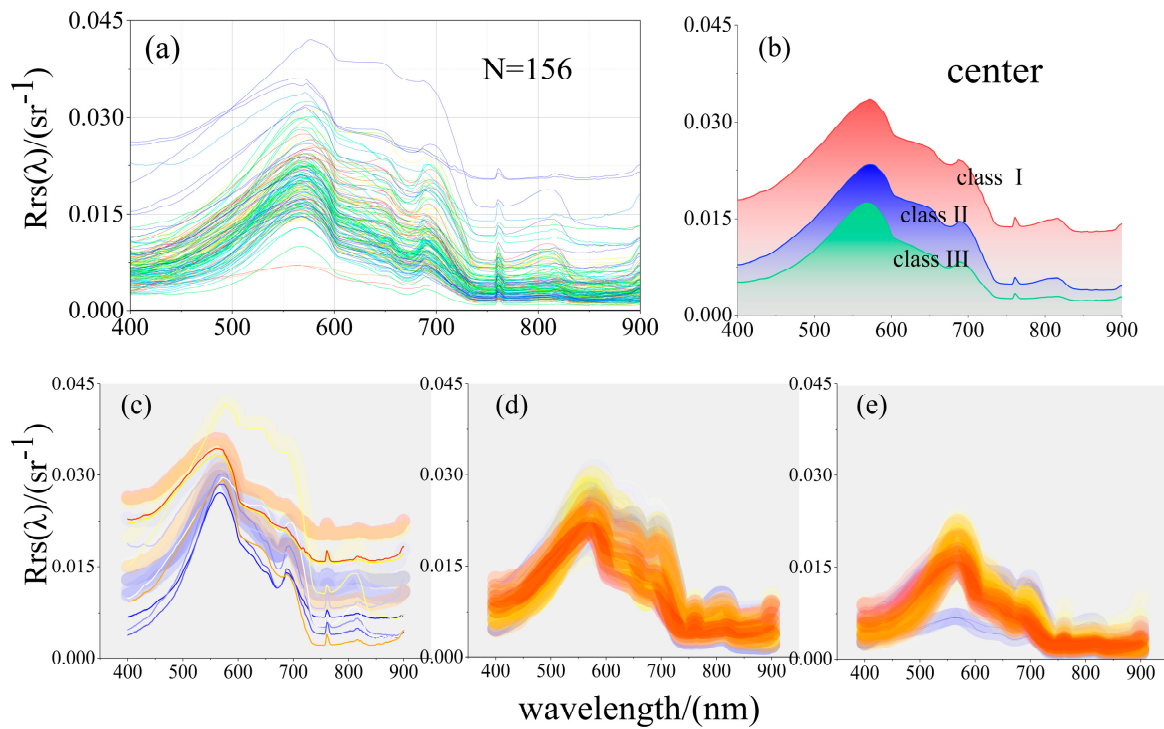| Methods	Class	x	Model	R^2
No classification	NCM	Rrs (665)/Rrs (490)	−44.58 ∗ x + 103.23	0.74
classification	class I	Rrs (665)/Rrs (443)	43.08 ∗ x + 2.99	0.80
	class II	Rrs (665)/Rrs (490)	49.06 ∗ x + 8.49	0.83
	class III	Rrs (705)/Rrs (490)	25.31 ∗ x + 30.29	0.74

Figure 3. Classification of measured remote sensing reflectance classification. (**a**) The distribution of all spectral data. (**b**) The central spectrum of each of the three classes after performing fuzzy classification on all spectral data. (**c–e**): The distribution of spectral data for the three groups, with sample sizes of 9, 54, and 93, respectively.

4.2.1. Unclassified Case

Utilizing data collected on 14 June, 21 July, 24 August, 17 September, 12 October 2020, and 29 June 2021, 156 sets of measured parameters were employed to calculate the comprehensive nutrient status index and identify the optimal band ratio (Rrs (665)/Rrs (490)) for the NCM evaluation model, as presented in Table 1. A comparison was conducted between the measured TSI and the model–inverted TSI, yielding an accuracy of $R^2 = 0.74$ (Figure 4).
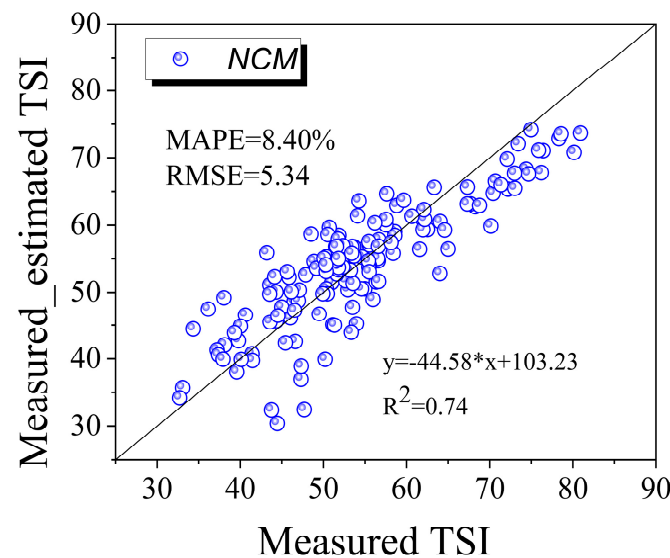

Figure 4. Accuracy test of the NCM method.

4.2.2. FCM Classification

Assessment models for the three water types were established using the optimal band ratios of Rrs, as outlined in Table 1. The empirical models for Classes 1, 2, and 3 demonstrated commendable accuracy, with R^2 values of 0.74, 0.80, and 0.83, respectively. A comparison between the measured TSI and TSI derived through the FCM yielded an accuracy of $R^2 = 0.85$ (Figure 5). Notably, the classification-based inversion models exhibited markedly enhanced accuracy compared with the NCM method, imparting heightened reliability and credibility to the findings.
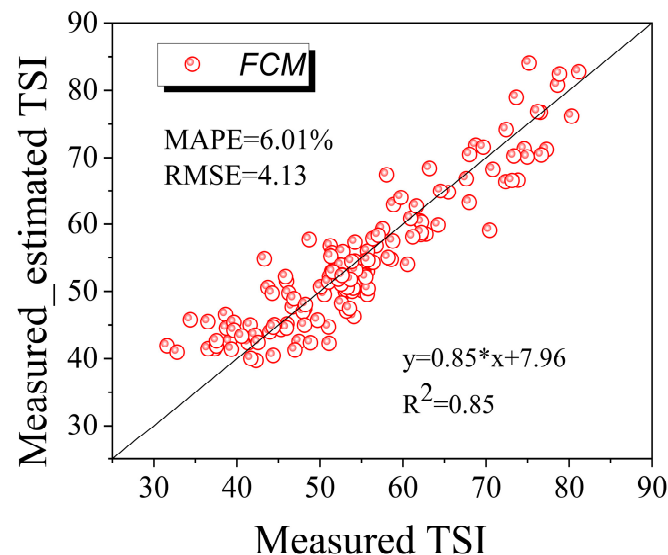
Figure 5. Accuracy test of the FCM method.

4.3. Evaluation of TSI Inversion Results Based on MSI Data

4.3.1. Verification of MSI Atmospheric Correction

The atmospheric correction of the MSI data was validated using in-situ measured spectral data, as illustrated in Figure 6. From Figure 6a–c, there is substantial agreement between the measured and Sentinel-2 MSI spectral reflectance on 14 June 2020, 19 July 2020, and 12 October 2020 ($R^2 = 0.91$, RMSE = 0.003 sr^{-1}, MAPE = 28.05%; $R^2 = 0.78$, RMSE = 0.003 sr^{-1}, MAPE = 26.25%; and $R^2 = 0.65$, RMSE = 0.004 sr^{-1}, MAPE = 30.44%). These results demonstrate the credibility of the atmospheric correction results for MSI data, establishing their suitability for subsequent retrieval applications.

4.3.2. Verification of TSI Results from MSI Inversion

The TSI results obtained through the non–classification and fuzzy classification methods were assessed using the three MSI images mentioned earlier. Figure 7 illustrates a visual representation of the accuracy achieved by both methods. The non–classification method yielded an R^2 of 0.49, RMSE of 6.88, and MAPE of 10.36%. Conversely, the fuzzy classification method demonstrated enhanced retrieval accuracy with an R^2 of 0.55, RMSE of 8.89, and MAPE of 13.18%. Although the improvement of the FCM method over the NCM method is not substantial, there is still a noticeable enhancement in the results (Figure 7). The results also indicate the potential of the fuzzy−classification-based approach to significantly improve the precision of nutrient status retrieval. The full scope of application and development potential for nutrient status remote sensing assessment through fuzzy classification remains an area that warrants further exploration.
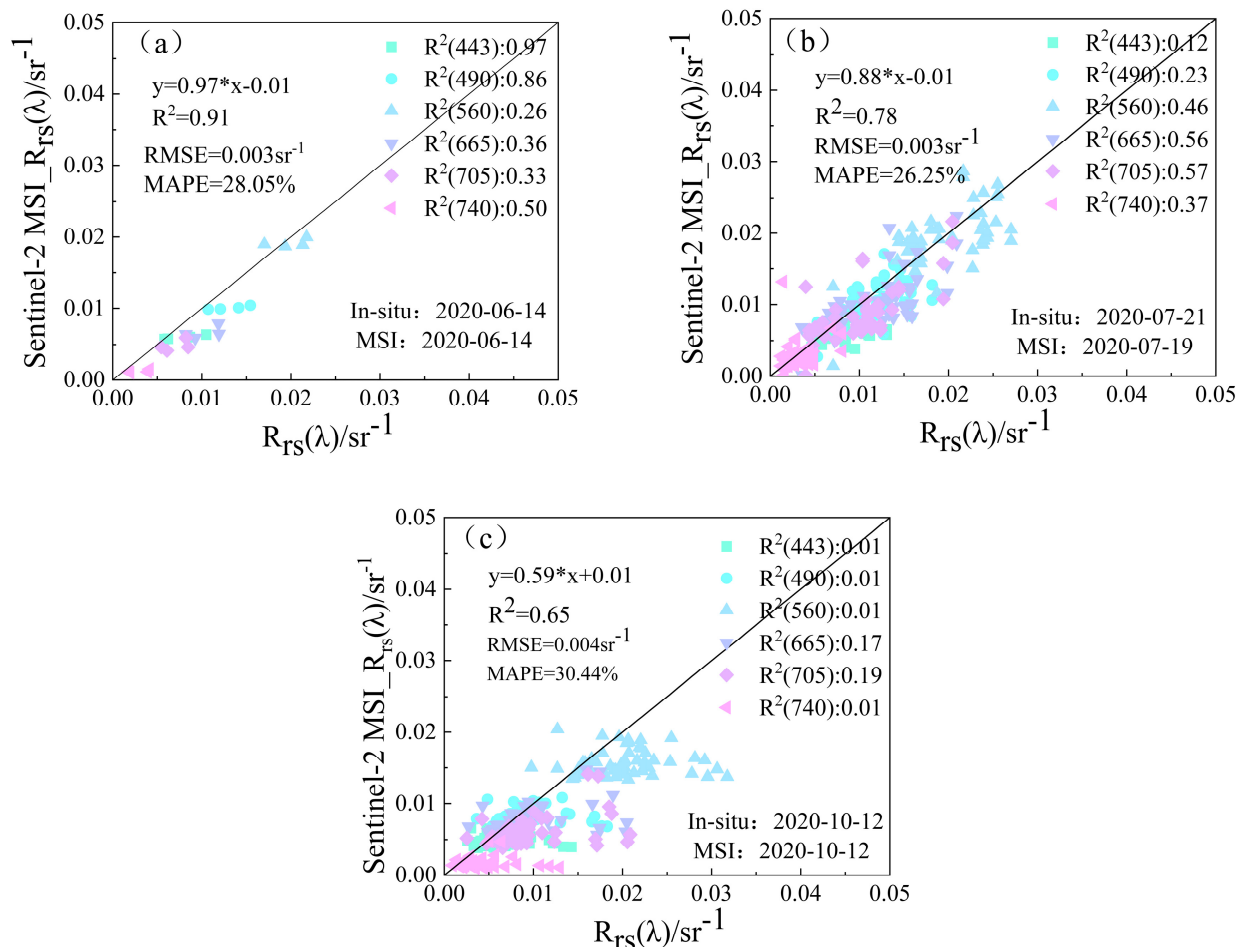
Figure 6. Atmospheric correction.Comparison of in-situ measured reflectance and satellite-derived reflectance for different dates at the site.
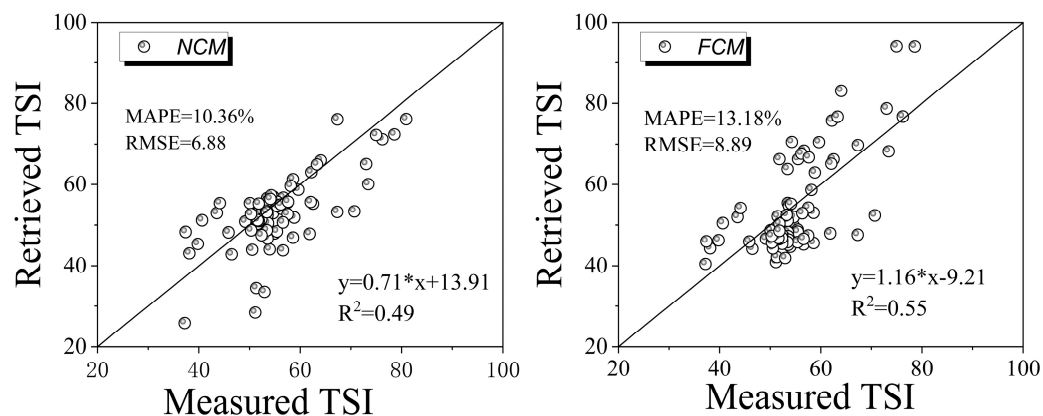

Figure 7. Comparison of in situ TSI and remote sensing retrieval.

4.3.3. Remote Sensing Application

Utilizing 156 sets of satellite–ground synchronized data obtained from Lake Daihai, optimal band ratio linear algorithms were developed for both the hard classification and fuzzy classification methods (Table 1). Subsequently, empirical models were applied to synchronized remote sensing images captured on 14 June, 19 July, and 12 October 2020 (Figure 8).
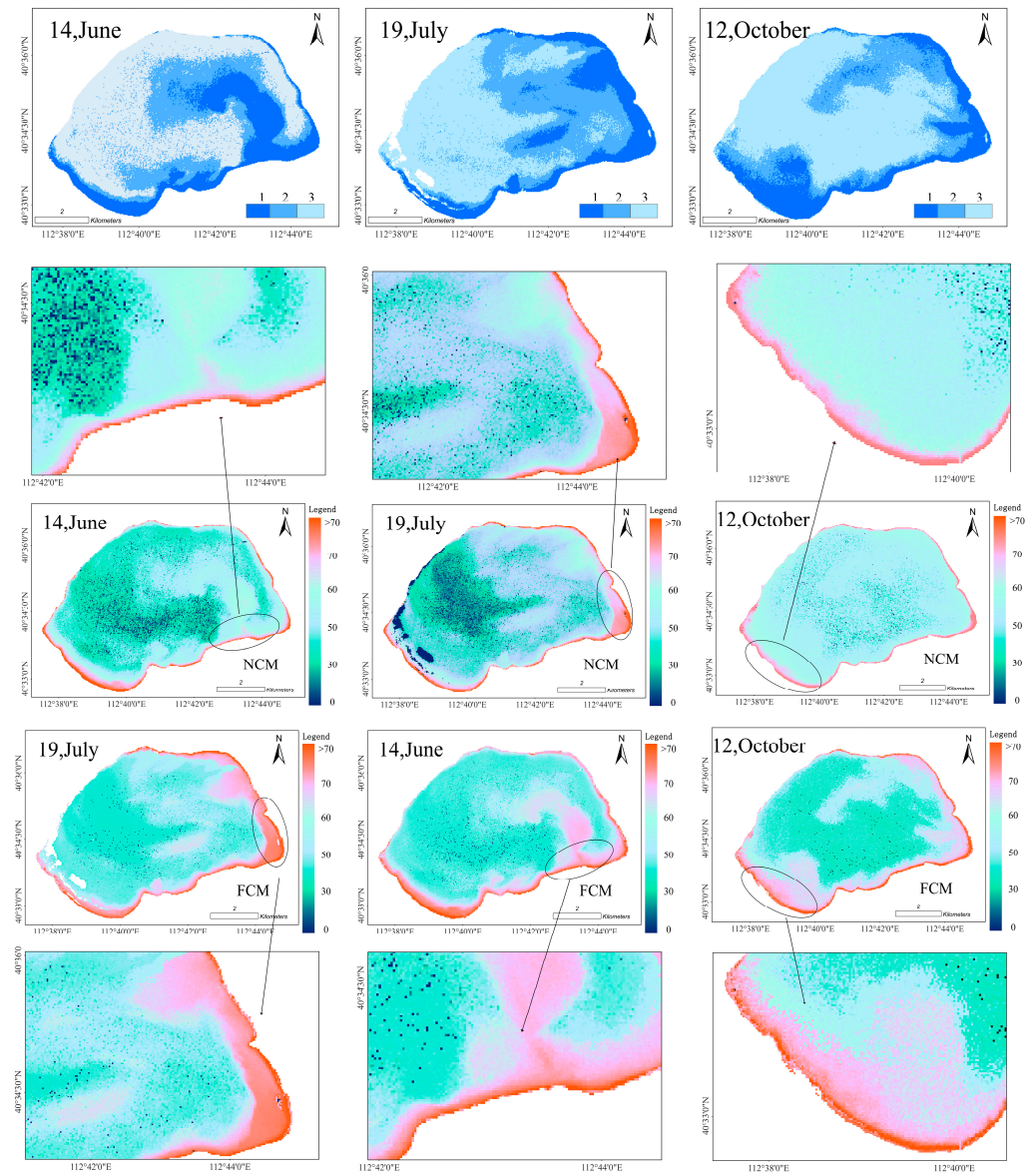
Figure 8. Optical classification and model application of remote sensing image water bodies. The black circles highlights the regions where differences exist between the two images.

First, fuzzy–classification-based optical classification was applied to remote sensing images of water bodies, as illustrated in the upper section of Figure 8. The classification graph in Figure 2 indicates that water type 1, characterized by the highest remote sensing reflectance, predominantly appeared at the lake boundaries, followed by other types, with type 3 covering the largest area. Subsequently, the same images were employed for eutrophication inversion using the non-classification method (NCM). The magnified view of Figure 8 reveals that the NCM method produces more distinct boundaries in the eutrophic areas (severe eutrophication: TSI > 70, moderate eutrophication: TSI > 60), while the FCM method displays smoother transitions, particularly in the more vividly colored regions. The differences between these two methods are primarily observed in the eutrophic zones, with minimal variations in other areas. Eutrophication in water bodies is a natural phenomenon that typically lacks distinct boundaries, highlighting the limitations of the NCM method. In contrast, the black line shows a smooth transition in nutrient levels along the water body boundaries, indicating that the fuzzy classification method effectively reduces discontinuities at the water type boundaries. The eutrophication areas during the three image periods were relatively small and were primarily located near the water–land

boundary. This phenomenon may be attributed to the increased suspended matter in the water due to sediment influx, resulting in higher reflectance and poorer nutrient status. A comparative analysis between the two methods revealed that the nutrient status assessment based on NCM was underestimated compared to the fuzzy classification method.

4.4. Spatial and Temporal Distribution Characteristics and Influencing Factors of Daihai TSI
4.4.1. Monthly Variation

Utilizing a time series of Sentinel-2 MSI remote sensing images, an FCM–based nutrient status classification method was employed to estimate the eutrophication levels of Lake Daihai from April to October. Annual spatial distribution maps of nutrient status were generated by dividing the images for the respective months by the total count (Figure 9). The monthly nutrient status maps revealed that in April, May, and October, Lake Daihai exhibited eutrophication primarily in the southern region. However, from June to September, the water quality was generally excellent, with the majority of water bodies experiencing mild eutrophication.
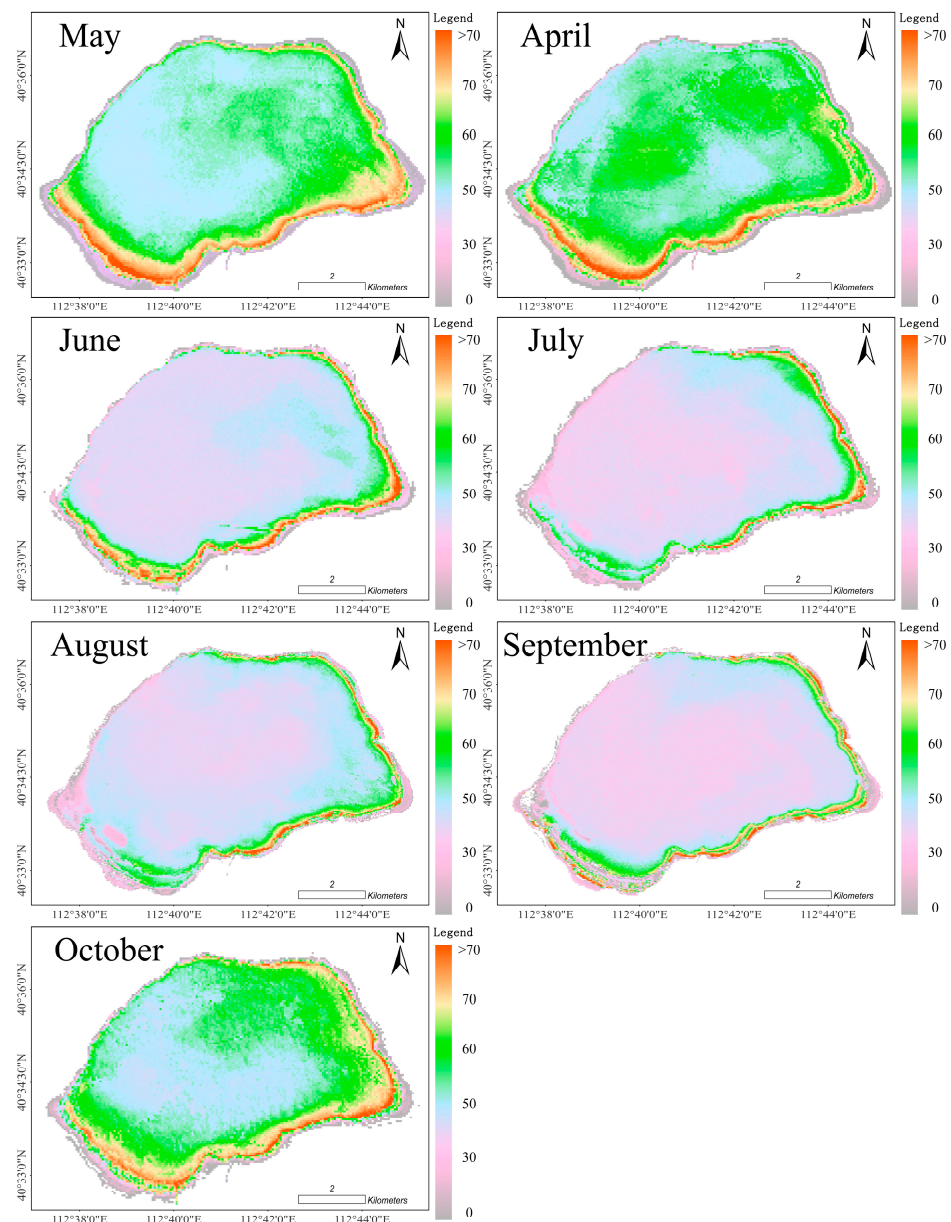

Figure 9. TSI monthly spatial variation.

4.4.2. Interannual Variation

Figure 10 illustrates the annual dynamics of the nutrient status. In 2016, the water body experienced the most severe eutrophication, followed by that in 2017, with pronounced eutrophication observed in the southern and southeastern parts of the lake. In 2018 and 2019, the water quality was excellent, with only limited signs of eutrophication. In 2020 and 2021, eutrophication was evident around the lakeshore. Generally, from 2016 to 2021, severe eutrophication is predominantly concentrated near the water-land boundary. Eutrophication gradually extended from the lake shore towards the lake surface, with the majority of the lake surface characterized by a mild to moderate nutrient status.
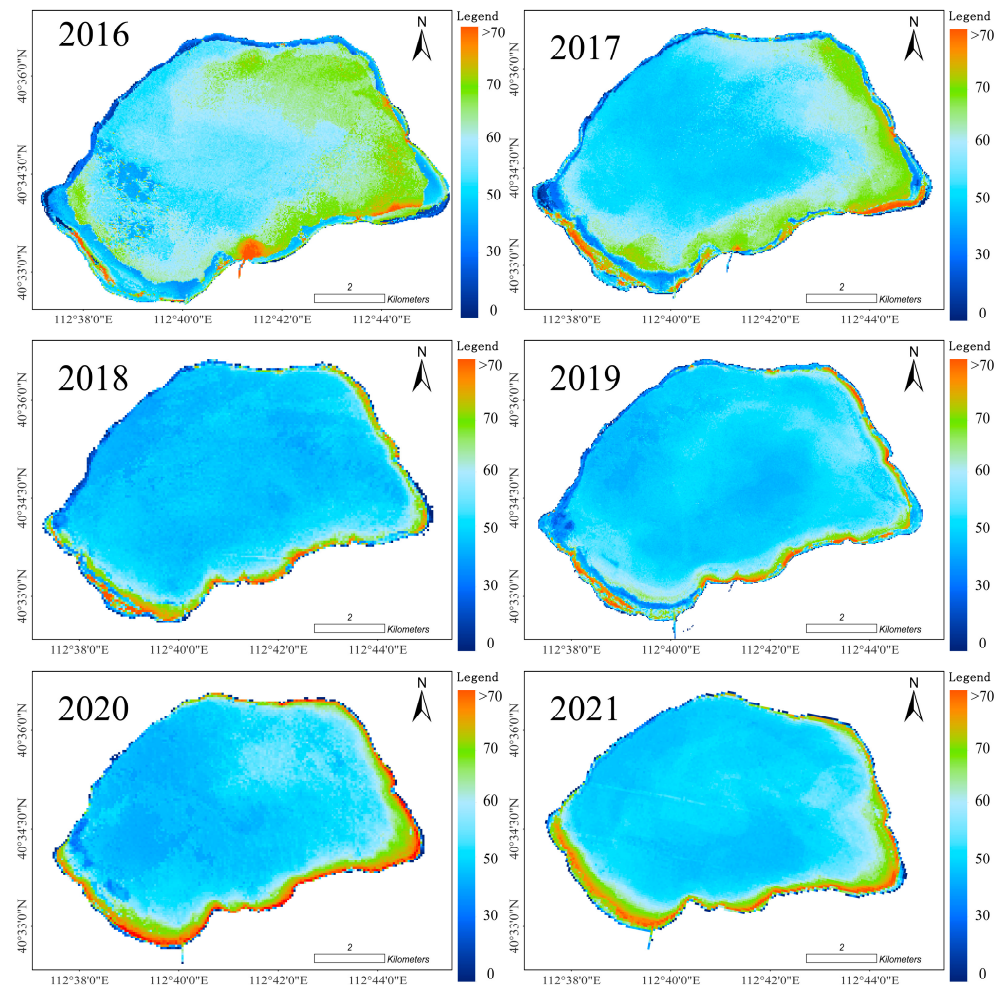

Figure 10. TSI annual spatial variation.

4.4.3. Analysis of Influencing Factors

Structural equation models find extensive applications across various domains [57,58]. Typically, climate change has a notable short–term impact, whereas human activities have a long-term influence. Therefore, as depicted in Figure 11, this study conducted climate factor analysis concerning monthly fluctuations in the nutrient status of Lake Daihai, along with an examination of agricultural and industrial factors on an interannual scale. The meteorological factors exhibited a significant impact on the monthly variations in the nutrient status of Lake Daihai, with a commendable goodness–of–fit for the structural equation model at 94%. Interannual fluctuations in nutrient status demonstrated a strong correlation with agricultural and industrial factors, accounting for 86% and 76% of the influence, respectively. Hence, human-related factors constituted the primary driver of eutrophication in Lake Daihai over an extended temporal horizon.
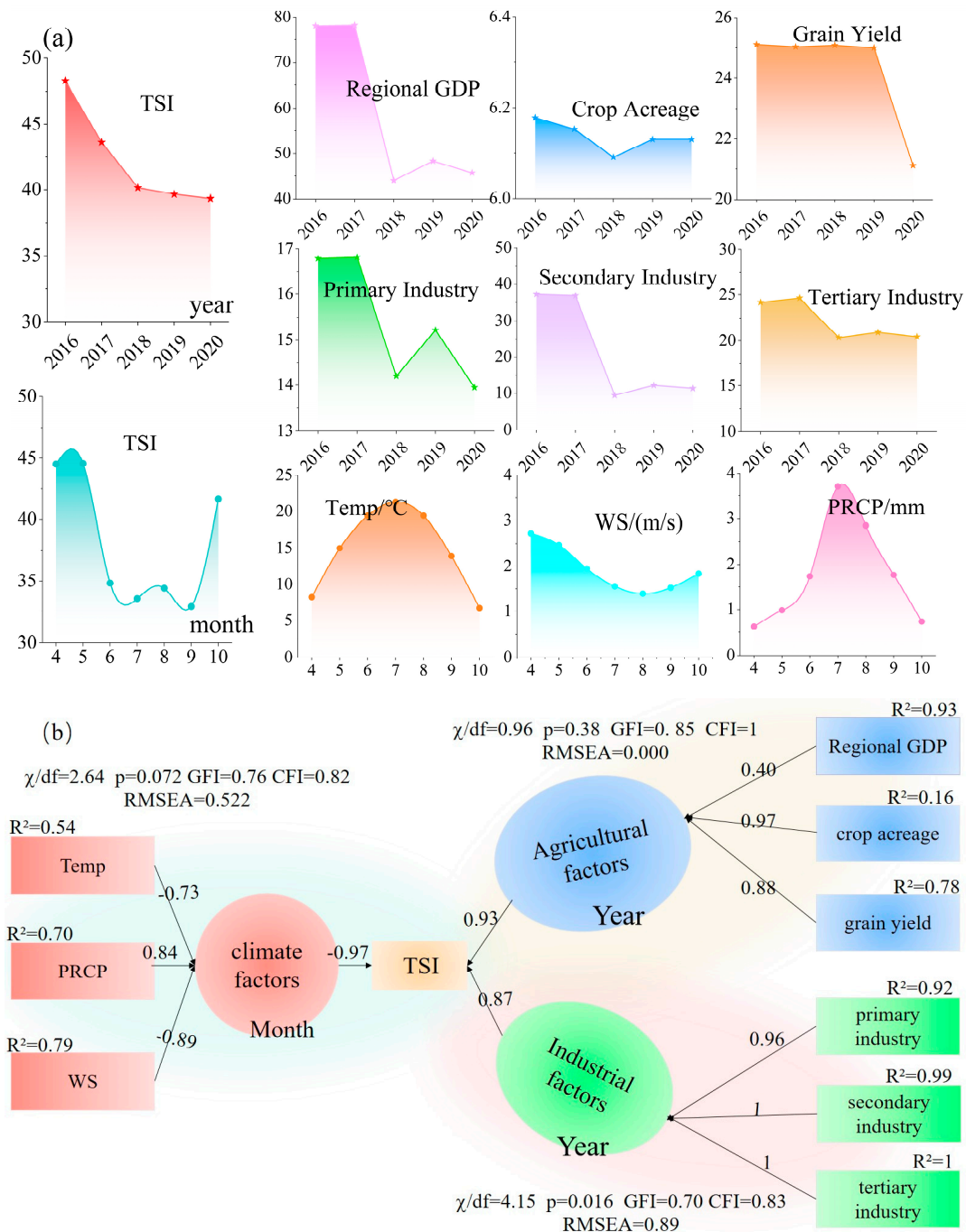
Figure 11. Trend analysis of factors influencing trophic status (**a**) and structural equation models (**b**).

In April and May, high wind speeds can easily disturb the sediment at the bottom of the lake, leading to the suspension and release of nutrients. Additionally, strong winds can disrupt the surface of Daihai Lake, causing sediment–laden water to be pushed into the lake, which in turn results in changes to the trophic state. Starting in June, wind speeds significantly decrease and temperatures gradually rise, creating favorable conditions for the growth of aquatic plants. By October, the growth of these plants reaches its peak, further exacerbating the eutrophication of the lake. Since 2017, the environmental conditions of the water area have improved, primarily due to the implementation of the "Ulanqab City Regulations on the Protection of Daihai and Huangqihai Lakes" and the shutdown of the Daihai Water Cooling Power Plant in 2018, among other measures [59].

5. Discussion

5.1. Sensibility Analysis

The FCM algorithm has been applied to various classification studies, ranging from medical image processing to remote sensing [60], and has shown extensive applications in fields such as image analysis, medical diagnosis, shape analysis, and target recognition [61]. In FCM clustering, parameters such as m, ε, and T are conventionally set to their default values except for the determination of the cluster count. Based on previous studies on the Daihai water body, which is characterized by predominantly singular spectral types, empirical analysis has established the optimal cluster count as n = 3. In most studies, FCM applications tend to employ the default value of the weighted exponent, m = 2, recognized as the exponent weight employed to effectively "balance" noise in the data [62]. FCM converges to hard clustering (HCM) as m approaches 1, while the singular solution of FCM converges to the centroid of the dataset as m approaches infinity [63]. Nevertheless, despite the acknowledged significance of the fuzzy parameter m in FCM clustering and the recognition that the preset value may not be universally suitable for all water body types, detailed guidelines for discerning an appropriate m value tailored to diverse datasets, particularly within the context of the optical clustering of water bodies, are currently lacking.

In this study, the determination of the fuzzy parameter, denoted as "m", was omitted when employing the FCM clustering method for the optical classification of water bodies. Dembele et al. [64] have elucidated that the level of fuzziness in FCM is contingent upon the fuzzy parameter "m" and the matrix norm "A", indicating the significance of optimizing "m" to augment the fuzziness of FCM. Furthermore, other researchers have proposed that the selection of the weighted exponent relies on the inherent characteristics of the data, with the optimal value of "m" exhibiting substantial variability across distinct datasets [64,65]. Additionally, Bi et al. (2019) [39] noted that employing the default value of "m = 2", especially in the context of high-dimensional data, may result in increased misclassifications of categorical objects and insufficient separation of spectra containing vegetation. Therefore, they proposed an adaptive algorithm termed FCM–m, founded on a dataset of inland water bodies in China, and the outcomes demonstrated its superior efficacy compared with the conventional FCM algorithm.

To apply FCM effectively in eutrophic lakes, it is crucial to engage in rigorous theoretical research to determine the optimal value of "m", which is dependent on the intrinsic data characteristics. Based on the examination of membership distribution at different "m" values in Figure 12 and the findings of Bi et al. (2019) [39], this study selected "m" values of 1.1, 1.36, 2, 3.6, and 5.6. When m = 1.1 and 1.36, the class members exhibited a pronounced concentration at the ends, with relatively fewer interconnections in the middle. This pattern suggests robust associations between the majority of the spectra and their respective clusters. In contrast, for m = 3.6 and 5.6, the membership degrees tended to converge towards the center, indicating a lack of distinct affiliations with any particular cluster. Among these values, m = 2 proved to be the most suitable choice for fuzzy clustering of the water body spectra. It adeptly assigned the majority of the spectra to specific clusters while simultaneously achieving a commendable balance for those that were less accurately classified.

5.2. Applicability of the Model

Human activities play a significant role in influencing the nutrient levels of water bodies. Studies have indicated that early stage developments, including the construction of small–to medium–sized reservoirs in the Daihai Basin and extensive agricultural expansion, led to wetland conversion for farmland and pastures. This has resulted in amplified cultivated land and an upswing in the agricultural population. However, due to intensified agricultural irrigation, increased industrial water consumption, excessive groundwater extraction, and reduced surface area coverage, Daihai's water level has rapidly declined. This has contributed to heightened nutrient concentrations and deterioration of the nutrient status [66–68]. The findings of this study have broad implications for water resource

management and environmental policy–making. By combining optical classification with the Trophic State Index (TSI) method, the accuracy of eutrophication assessments has been enhanced, providing more reliable data for decision–makers to develop targeted strategies for lake restoration and protection. This approach can aid in mitigating eutrophication issues, improving water quality, and ensuring the sustainable use of water resources in areas affected by both anthropogenic and natural pressures.
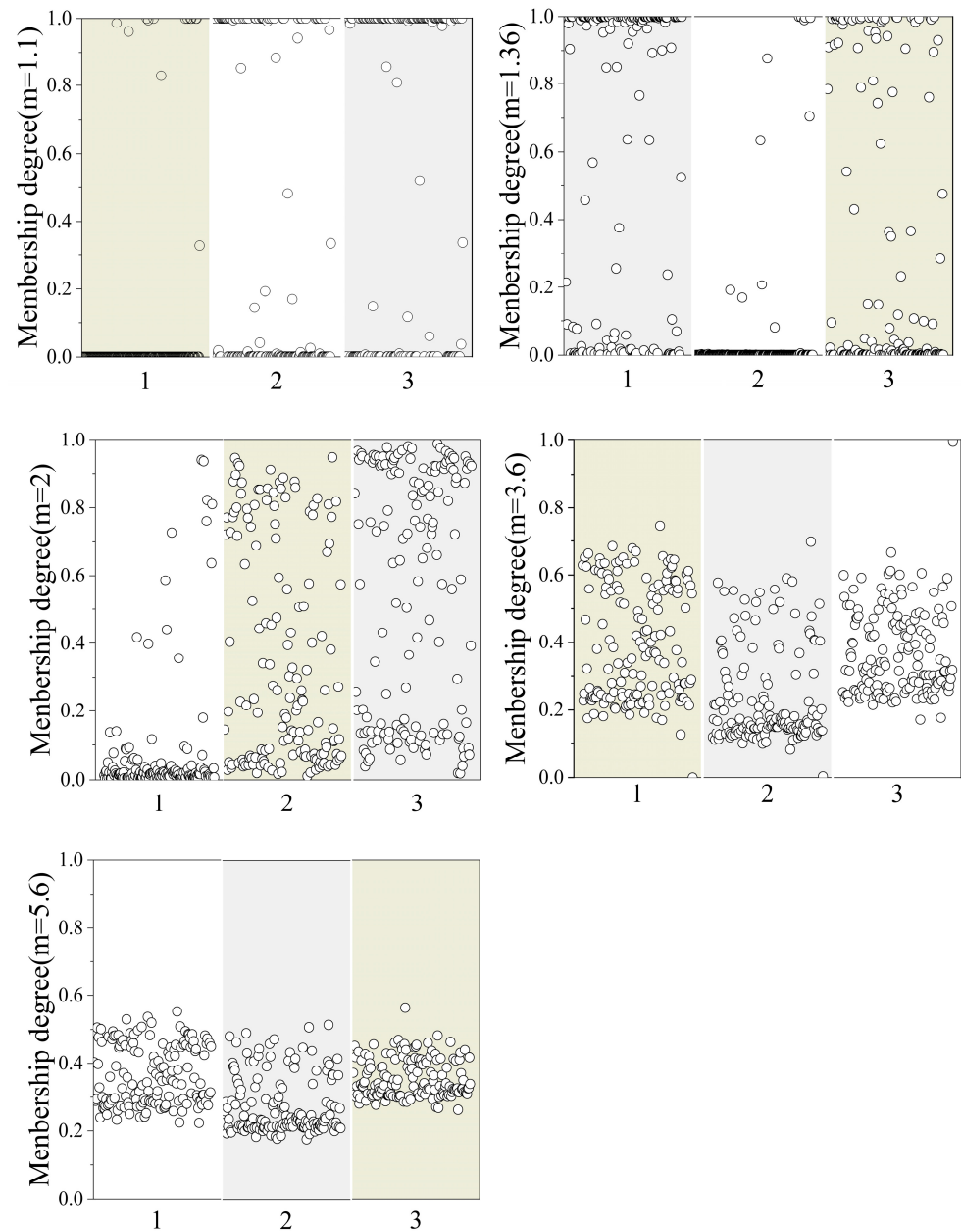

Figure 12. Distribution of membership degree from fuzzy clustering algorithms. The horizontal axis represents the water body types.

Currently, recognizing the complexity of water optical properties and its limitations on estimating Chla from remote sensing data, many researchers have conducted optical classifications of coastal and inland waters [33,35,37]. Based on different water types, specific Chla estimation algorithms have been developed, leading to hybrid algorithms for Chla estimation. Most research findings suggest that optical classification of water bodies can significantly improve the performance of Chla estimation algorithms [21]. Building on these studies, the approach of performing optical classifications of complex waters

to develop specific algorithms is equally applicable to estimating water eutrophication. In this context, soft classification methods play a crucial role by enabling more flexible categorization of water bodies, reflecting the continuous variation of water properties rather than rigidly assigning them to a single category. Similar optical classification methods have been successfully applied to various water bodies globally, ranging from tropical lakes to temperate and subarctic waters, demonstrating broad applicability. Therefore, we have reason to believe that this approach can be used to develop more precise models for assessing eutrophication, offering enhanced accuracy. However, when this method is applied to regions with significantly different environmental conditions, it may encounter certain limitations. Therefore, careful adjustments and optimizations of the model are necessary to ensure its suitability for specific regions.

6. Conclusions

This study integrated fuzzy classification techniques with nutrient status index methodologies, employing measured spectra, transparency, and chlorophyll data to evaluate the nutrient status of the Daihai Lake. A tailored nutrient status assessment model for Daihai Lake was developed.

(1) Fuzzy classification techniques were employed to categorize the in situ remote sensing reflectance, resulting in the identification of three spectral classes characterized by distinctive feature disparities.

(2) Empirical models were developed for the NCM and FCM methods using the measured data. Optimal band ratios were selected to establish the models, yielding inversion accuracy test results of $R^2 = 0.74$ and $R^2 = 0.85$, respectively. Fuzzy clustering demonstrated the potential for evaluating the nutrient status of water bodies.

(3) Atmospheric correction of the three synchronized field images was successfully validated. The accuracy assessment of the remote sensing inversion using the NCM and FCM methods yielded the following results: $R^2 = 0.49$, RMSE = 6.88, MAPE = 10.36%, and $R^2 = 0.55$, RMSE = 8.89, MAPE = 13.18%.

(4) The algorithm was applied to Sentinel MSI remote sensing images to analyze the temporal and spatial distribution characteristics of the trophic status of the Daihai Reservoir from April to October from 2016 to 2021. MSI time-series data revealed a long-term state of mild eutrophication in Daihai. The primary factors underlying eutrophication were elucidated using a structural equation model. Climate-related factors accounted for 94% of the monthly variation in the trophic status of the Daihai Reservoir, while agricultural and industrial factors exhibited significant correlations with interannual variations, explaining 86% and 76% of the variations, respectively. This highlights the predominant role of human activities in the eutrophication of the Daihai Reservoir, with climate factors acting as catalysts.

Author Contributions: Data curation, Q.L.; Writing—original draft, F.W.; Writing—review & editing, S.Q.; Supervision, C.S. and A.C.; Funding acquisition, S.Q. All authors have read and agreed to the published version of the manuscript.

Data Availability Statement: The data presented in this study are available on request from the corresponding author due to as it involves the privacy of the participants and is therefore not publicly disclosed in the article.

Conflicts of Interest: The authors declare that they have no known competing financial interests or personal relationships that could have appeared to influence the work reported in this paper.

References

1. Dhillon, J.K.; Mishra, A.K. Estimation of Trophic State Index of Sukhna Lake Using Remote Sensing and GIS. *J. Indian Soc. Remote Sens.* **2013**, *42*, 469–474. [CrossRef]
2. Hu, M.; Ma, R.; Xue, K.; Cao, Z.; Xiong, J.; Loiselle, S.A.; Hou, X. Eutrophication evolution of lakes in China: Four decades of observations from space. *J. Hazard. Mater.* **2024**, *470*, 134225. [CrossRef] [PubMed]
3. Orlandi, C.; Blasutto, O.; Pittaluga, F.; Bettoso, N.; Acquavita, A. Seasonal and interannual variability of the trophic state in the marano and Grado lagoon (adriatic sea, italy) during the 2011–2021 period. *Environments* **2024**, *11*, 152. [CrossRef]
4. Dodds, W.K. Trophic state, eutrophication and nutrient criteria in streams. *Trends Ecol. Evol.* **2007**, *22*, 669–676. [CrossRef]
5. Carlson, R. A trophic state index for lakes 1. *Limnol. Oceanogr.* **1977**, *22*, 361–369. [CrossRef]
6. Cheng, K.S.; Lei, T.C. Reservoir Trophic State Evaluation Using Lanisat Tm Images. *J. Am. Water Resour. Assoc.* **2001**, *37*, 1321–1334. [CrossRef]
7. Iwashita, K.; Kudoh, K.; Fujii, H.; Nishikawa, H. Satellite analysis for water flow of Lake Inbanuma. *Adv. Space Res.* **2004**, *33*, 284–289. [CrossRef]
8. Wezernak, C.T.; Tanis, F.J.; Bajza, C.A. Trophic state analysis of inland lakes. *Remote Sens. Environ.* **1976**, *5*, 147–164. [CrossRef]
9. Jally, S.K.; Mishra, A.K.; Balabantaray, S. Estimation of Trophic State Index of Chilika Lake using Landsat-8 OLI and LISS-III satellite data. *Geocarto Int.* **2018**, *35*, 759–780. [CrossRef]
10. Wang, Z.J.; Hong, J.M.; Du, G.S. Use of satellite imagery to assess the trophic state of Miyun Reservoir, Beijing, China. *Environ. Pollut.* **2008**, *155*, 13–19.
11. Hu, M.; Ma, R.; Cao, Z.; Xiong, J.; Xue, K. Remote Estimation of Trophic State Index for Inland Waters Using Landsat-8 OLI Imagery. *Remote Sens.* **2021**, *13*, 1988. [CrossRef]
12. Duan, H.; Zhang, Y.; Zhang, B.; Song, K.; Wang, Z. Assessment of Chlorophyll-a Concentration and Trophic State for Lake Chagan Using Landsat TM and Field Spectral Data. *Environ. Monit. Assess.* **2006**, *129*, 295–308. [CrossRef] [PubMed]
13. Olmanson, L.G.; Bauer, M.E.; Brezonik, P.L. A 20-year Landsat water clarity census of Minnesota's 10,000 lakes. *Remote Sens. Environ.* **2008**, *112*, 4086–4097. [CrossRef]
14. Mishra, A.K.; Garg, N. Analysis of Trophic State Index of Nainital Lake from Landsat −7 ETM Data. *J. Indian Soc. Remote Sens.* **2011**, *39*, 463–471. [CrossRef]
15. Song, K.S.; Li, L.; Li, S.; Tedesco, L.; Hall, B.; Li, L. Hyperspectral Remote Sensing of Total Phosphorus (TP) in Three Central Indiana Water Supply Reservoirs. *Water Air Soil Pollut.* **2011**, *223*, 1481–1502. [CrossRef]
16. Qin, B.Q.; Gao, G.; Zhu, G.W.; Zhang, Y.L.; Song, Y.Z.; Tang, X.M.; Hai, X.U. Lake eutrophication and its ecosystem response. *Chin. Sci. Bull.* **2012**, *58*, 961–970. [CrossRef]
17. Sun, D.; Qiu, Z.F.; Li, Y.M.; Shi, K.; Gong, S. Detection of Total Phosphorus Concentrations of Turbid Inland Waters Using a Remote Sensing Method. *Water Air Soil Pollut.* **2014**, *225*, 1–17. [CrossRef]
18. Eraso, R.; Galo, M.D.L.; Alcântara, E.; Shimabukuro, M.; Carmo, A. Locally tuned model to map the chlorophyll-a and the trophic state in Porto Primavera reservoir using MODIS/Terra images. *Model. Earth Syst. Environ.* **2018**, *4*, 39–47. [CrossRef]
19. Liu, Y.; Wu, H.; Gao, H.; Guo, P. Evaluation of trophic state for inland waters through combining Forel-Ule Index and inherent optical properties. *Sci. Total Environ.* **2022**, *820*, 153316. [CrossRef]
20. Zhang, Y.; Zhou, Y.; Shi, K.; Qin, B.; Yao, X.; Zhang, Y. Optical properties and composition changes in chromophoric dissolved organic matter along trophic gradients: Implications for monitoring and assessing lake eutrophication. *Water Res.* **2018**, *131*, 255–263. [CrossRef]
21. Shi, K.; Zhang, Y.; Song, K.; Liu, M.; Zhou, Y.; Zhang, Y.; Li, Y.; Zhu, G.; Qin, B. A semi-analytical approach for remote sensing of trophic state in inland waters: Bio-optical mechanism and application. *Remote Sens. Environ.* **2019**, *232*, 111349. [CrossRef]
22. Wen, Z.; Song, K.; Liu, G.; Shang, Y.; Fang, C.; Du, J.; Lyu, L. Quantifying the trophic status of lakes using total light absorption of optically active components. *Environ. Pollut.* **2019**, *245*, 684–693. [CrossRef] [PubMed]
23. Wang, S.; Li, J.; Zhang, B.; Spyrakos, E.; Tyler, A.N.; Shen, Q.; Zhang, F.F.; Kuster, T.; Lehmann, M.K.; Wu, Y.H.; et al. Trophic state assessment of global inland waters using a MODIS-derived Forel-Ule index. *Remote Sens. Environ.* **2018**, *217*, 444–460. [CrossRef]
24. Chen, Q.; Huang, M.; Tang, X. Eutrophication assessment of seasonal urban lakes in China Yangtze River Basin using Landsat 8-derived Forel-Ule index: A six-year (2013–2018) observation. *Sci. Total Environ.* **2020**, *745*, 135392. [CrossRef]
25. Guan, Q.; Feng, L.; Hou, X.; Schurgers, G.; Zheng, Y.; Tang, J. Eutrophication changes in fifty large lakes on the Yangtze Plain of China derived from MERIS and OLCI observations. *Remote Sens. Environ.* **2020**, *246*, 111890. [CrossRef]
26. Watanabe, F.S.Y.; Miyoshi, G.T.; Rodrigues, T.W.P.; Bernardo, N.M.R.; Imai, N.N. Inland water's trophic status classification based on machine learning and remote sensing data. *Remote Sens. Appl. Soc. Environ.* **2020**, *19*, 100326. [CrossRef]
27. Werther, M.; Spyrakos, E.; Simis, S.G.H.; Odermatt, D.; Tyler, A. Meta-classification of remote sensing reflectance to estimate trophic status of inland and nearshore waters. *ISPRS J. Photogramm. Remote Sens.* **2021**, *176*, 109–126. [CrossRef]
28. Hu, M.; Ma, R.; Xiong, J.; Wang, M.; Cao, Z.; Xue, K. Eutrophication state in the Eastern China based on Landsat 35-year observations. *Remote Sens. Environ.* **2022**, *277*, 113057. [CrossRef]
29. Javaid, M.; Shafi, A.; Hamid, A.; Jehangir, A.; Yousuf, A.R. Dynamics of the wetland ecosystem health in urban and rural settings in high altitude ecoregion. *Sci. Total Environ.* **2023**, *904*, 166566. [CrossRef]
30. Mukonza, S.S.; Chiang, J.L. Machine and deep learning-based trophic state classification of national freshwater reservoirs in taiwan using sentinel-2 data. *Phys. Chem. Earth* **2024**, *134*, 103541. [CrossRef]

31. Lubac, B.; Loisel, H. Variability and classification of remote sensing reflectance spectra in the eastern English Channeland southern North Sea. *Remote Sens. Environ.* **2007**, *110*, 45–58. [CrossRef]

32. Vantrepotte, V.; Loisel, H.; Dessailly, D.; Mériaux, X. Optical classification of contrasted coastal waters. *Remote Sens. Environ.* **2012**, *123*, 306–323. [CrossRef]

33. Bao, Y.; Tian, Q.; Chen, M. A Weighted Algorithm Based on Normalized Mutual Information for Estimating the Chlorophyll-a Concentration in Inland Waters Using Geostationary Ocean Color Imager (GOCI) Data. *Remote Sens.* **2015**, *7*, 11731–11752. [CrossRef]

34. Zhang, F.F.; Li, J.S.; Shen, Q.; Zhang, B.; Wu, C.Q.; Wu, Y.F.; Wang, G.L.; Wang, S.L.; Lu, Z.Y. Algorithms and schemes for chlorophyll a estimation by remote sensing and optical classification for Turbid Lake Taihu, China. *IEEE J. Sel. Top. Appl. Earth Observ. Remote Sens.* **2015**, *8*, 350–364. [CrossRef]

35. Zhang, F.; Li, J.; Shen, Q.; Zhang, B.; Tian, L.; Ye, H.; Wang, S.; Lu, Z. A soft-classification-based chlorophyll-a estimation method using meris data in the highly turbid and eutrophic taihu lake. *Int. J. Appl. Earth Obs. Geoinf.* **2019**, *74*, 138–149. [CrossRef]

36. Le, C.; Li, Y.; Zha, Y.; Sun, D.; Huang, C.; Zhang, H. Remote estimation of chlorophyll a in optically complex waters based on optical classification. *Remote Sens. Environ.* **2011**, *115*, 725–737. [CrossRef]

37. Shen, Q.; Li, J.; Zhang, F.; Sun, X.; Li, J.; Li, W.; Zhang, B. Classification of Several Optically Complex Waters in China Using in Situ Remote Sensing Reflectance. *Remote Sens.* **2015**, *7*, 14731–14756. [CrossRef]

38. Li, Y.; Wang, Q.; Wu, C.; Zhao, S.; Huang, C. Estimation of Chlorophyll a Concentration Using NIR/Red Bands of MERIS and Classification Procedure in Inland Turbid Water. *IEEE Trans. Geosci. Remote Sens.* **2012**, *50*, 988–997. [CrossRef]

39. Bi, S.; Li, Y.; Xu, J.; Liu, G.; Song, K.; Mu, M.; Lyu, H.; Miao, S.; Xu, J. Optical classification of inland waters based on an improved Fuzzy C-Means method. *Opt Express* **2019**, *27*, 34838–34856. [CrossRef]

40. Shi, K.; Li, Y.; Li, L.; Lu, H.; Song, K.; Liu, Z.; Xu, Y.; Li, Z. Remote chlorophyll-a estimates for inland waters based on a cluster-based classification. *Sci. Total Environ.* **2013**, *444*, 1–15. [CrossRef]

41. Fang, M.; Jinchao, F. Effects of Human Activities on Daihai Lake Inner Mongolia. *J. MUC (Nat. Sci. Ed.)* **2017**, *26*, 76–81.

42. Liu, X. Dynamic Change of Area and Water Level of Daihai Lake and Its Driving Force Analysis. Master's Thesis, Inner Mongolia University, Hohhot, China, 2019.

43. Zhou, Y.K.; Jiang, J.H.; Huang, Q. Water Quality Analysis and Assessment of Daihai Lake in Inner Mongolia. *J. Arid. Land Resoures Environ.* **2006**, 74–77. Available online: https://kns.cnki.net/kcms2/article/abstract?v=_kvDxI8xRKlhj6Xz-mjXU-qb5IpHb0 e2s5Y0PSXgrSmKusVOQIcjm0Om5ljvTVsmFG14w6fV5AasKkkJ4Ca1Gc5UC5wVkHzB7Hen_waY_J0SSPT1y1_oyzExBWIc8 KhRf8-xYgPqiGcExo_ygeqhKfWzfaLwHZ0DsjF8LEI2NeaLG_WuqtelkV3Ul64a-cdK&uniplatform=NZKPT&language=CHS (accessed on 27 August 2024).

44. Liang, X.; Liu, H.; Ji, M.; Chang, M. Effects of land use/cover change on lake water quality in the semi-arid region of northern China: A case study in Lake Daihai Basin (2000–2018). *Lake Sci.* **2021**, *33*, 727–738.

45. Tang, J.; Tian, G.; Wang, X.; Wang, X.; Song, Q. The Methods of Water Spectra Measurement and Analysis I: Above-Water Method. *J. Remote Sens.* **2004**, *8*, 37–44.

46. Bukata, R.P.; Jerome, J.H.; Bruton, J.E. Relationships among Secchi disk depth, beam attenuation coefficient, and irradiance attenuation coefficient for Great Lakes waters. *J. Great Lakes Res.* **1988**, *14*, 347–355. [CrossRef]

47. Jiang, G.; Loiselle, S.A.; Yang, D.; Ma, R. Remote estimation of chlorophyll a concentrations over a wide range of optical conditions based on water classification from VIIRS observations. *Remote Sens. Environ.* **2020**, *241*, 111735. [CrossRef]

48. Yang, H.; Song, J.; Teng, Y.; Song, X.; Zeng, P.; Jia, J. Coupling model-driven and data-driven methods for estimating soil moisture over bare surfaces with sentinel-1a dual-polarized data. *IEEE J. Sel. Top. Appl. Earth Obs. Remote Sens.* **2023**, *16*, 4820–4832. [CrossRef]

49. Ansper, A.; Alikas, K. Retrieval of Chlorophyll a from Sentinel-2 MSI Data for the European Union Water Framework Directive Reporting Purposes. *Remote Sens.* **2018**, *11*, 64. [CrossRef]

50. Neves, V.H.; Pace, G.; Delegido, J.; Antunes, S.C. Chlorophyll and Suspended Solids Estimation in Portuguese Reservoirs (Aguieira and Alqueva) from Sentinel-2 Imagery. *Water* **2021**, *13*, 2479. [CrossRef]

51. Brockmann, C.; Doerffer, R.; Peters, M.; Kerstin, S.; Embacher, S.; Ruescas, A. Evolution of the C2RCC Neural Network for Sentinel 2 and 3 for the Retrieval of Ocean Colour Products in Normal and Extreme Optically Complex Waters. EPASP 740. In Proceedings of the Living Planet Symposium 2016, Prague, Czech Republic, 9–13 May 2016.

52. Zadeh, L.A. Fuzzy sets as a basis for a theory of possibility. *Fuzzy Sets Syst.* **1978**, *1*, 3–28. [CrossRef]

53. Moore, T.S.; Campbell, J.W.; Hui, F. A fuzzy logic classification scheme for selecting and blending satellite ocean color algorithms. *IEEE Trans. Geosci. Remote Sens.* **2001**, *39*, 1764–1776. [CrossRef]

54. Zadeh, L.A. Fuzzy sets. *Inf. Control* **1965**, *8*, 338–353. [CrossRef]

55. Klir, G.J.; Yuan, B. *Fuzzy Sets and Fuzzy Logic*; Prentice Hall PTR 1-563; Prentice Hall: Hoboken, NJ, USA, 2011.

56. Hadjimitsis, D.G.; Clayton, C.R.I.; Toulios, L. A new method for assessing the trophic state of large dams in Cyprus using satellite remotely sensed data. *Water Environ. J.* **2010**, *24*, 200–207. [CrossRef]

57. Yang, R.M.; Guo, W.W.; Zheng, J.B. Soil prediction for coastal wetlands following spartina alterniflora invasion using sentinel-1 imagery and structural equation modeling. *Catena* **2019**, *173*, 465–470. [CrossRef]

58. Capellesso, E.S.; Cequinel, A.; Marques, R.; Marques, M.C.M. Temporal and environmental correlates of carbon stocks in a regenerating tropical forest. *Appl. Veg. Sci.* **2020**, *23*, 353–362. [CrossRef]

59. Ma, Q.; Wang, R.; Tan, R.J.; Cheng, J.; Wang, J. Remote Sensing Monitoring of Changes in Daihai Lake's Water Area and Volume Over the Past 40 Years. *Yellow River* **2022**, *44*, 57–59.

60. Moore, T.S.; Dowell, M.D.; Bradt, S.; Ruiz Verdu, A. An optical water type framework for selecting and blending retrievals from bio-optical algorithms in lakes and coastal waters. *Remote Sens. Environ.* **2014**, *143*, 97–111. [CrossRef]

61. Rezaee, M.R.; Lelieveldt, B.P.F.; Reiber, J.H.C. A new cluster validity index for the fuzzy c-mean. *Pattern Recognit. Lett.* **1998**, *19*, 237–246. [CrossRef]

62. Windham, M.P. Cluster validity for the fuzzy c-means clustering algorithrm. *IEEE Trans. Pattern Anal. Mach. Intell.* **1982**, *4*, 357–363. [CrossRef]

63. Yu, J.; Chen, Q.; Huang, H. Analysis of the weighting exponent in the FCM. *IEEE Trans. Syst. Man Cybern. B Cybern.* **2004**, *34*, 634–639. [CrossRef]

64. Dembele, D.; Kastner, P. Fuzzy C-means method for clustering microarray data. *Bioinformatics* **2003**, *19*, 973–980. [CrossRef] [PubMed]

65. Doulaye, D. Multi-objective optimization for clustering 3-way gene expression data. *Adv. Data Anal. Classif.* **2008**, *2*, 211–225.

66. Feng, X.W.; Wang, G.; Wang, Z.; Li, N. Analysis of Daihai Lake Inner Mongolia Water Resources. *J. China Hydrol.* **1994**, *1*, 55–56. [CrossRef]

67. Zhou, Y.; Jiang, J. Changes in the Ecological Environment in the Daihai Lake Basin Over the Years. *Aird Zone Res.* **2009**, *26*, 163–168.

68. Chen, H.; Fu, X.; Zhao, H.; Wang, G. Analysis on Climatic Influence of Ecological Environment Change of Daihai Lake wetland. *Meteorol. J. Inn. Mong.* **2011**, *6*, 14–17. [CrossRef]